Journal of Solid-Phase Biochemistry, Vol. 1, No. 1, 1976

VECTORIAL BEHAVIOR OF A HOMOGENEOUS ARTIFICIAL BIENZYME MEMBRANE

J. F. HERVAGAULT, M. C. DUBAN, J. P. KERNEVEZ, and D. THOMAS

Laboratoire de Technologie Enzymatique
Universite de Technologie de Compiègne
B.P. 233, 60206, Compiègne, France

Accepted January 13, 1976

Two sequential enzymes (xanthine oxidase and uricase) were immobilized in a homogeneous artificial membrane. The first substrate (xanthine) is a competitive inhibitor for the second enzyme (uricase). The paper deals with experimental and numerical results obtained with such a membrane studied under asymmetrical boundary conditions for the inhibitor (xanthine). Asymmetry at the boundaries gives rise to an asymmetrical function. In this way, a vectorial behavior of the global system is observed; urate concentration is increasing in the second compartment and decreasing in the first one. It is demonstrated that a pseudoactive transport is able to arise from a membrane symmetrical in structure when working under functional asymmetry.

INTRODUCTION

In this report, a study of a structural influence such as diffusion limitation on the kinetic behavior of a bienzyme system is presented. Artificially immobilized enzymes are a convenient tool for studying not only this structural influence in a simple context, but also enzyme behavior under asymmetrical conditions. Many studies deal with enzyme kinetics, but little attention has been paid to enzyme catalysis with asymmetrical boundary conditions. Blumenthal et al. (1) and David et al. (2) have described the reciprocal effect of enzyme reactions and membrane potential in artificial systems. A vectorial catalysis effect was observed by Broun et al. (3) with asymmetrically structured bienzyme membranes. The results to be presented here deal with a vectorial behavior of a homogeneous bienzyme membrane. Asymmetrical catalysis effects in chemical engineering were reviewed by Weisz (4).

Numerous reviews have been devoted to the subject of immobilized enzymes (5,6). In this study, the enzymes were immobilized with a previously described co–cross-linking method in a proteic membrane (7). Mosbach et al. (8–10) have immobilized several multienzyme systems onto particles and studied their kinetic behavior experimentally. Goldman and Katchalski (11) have published a numerical analysis of the kinetic behavior

of a bienzyme membrane, but without experimental results. Hervagault et al. (12) and Lecoq et al. (13) performed both experimental and numerical studies on bienzyme systems. All these studies were performed with symmetrical boundary conditions.

In our experimental system, xanthine oxidase is the first enzyme and uricase the second. Xanthine, the first substrate, is a competitive inhibitor of uricase.

MATERIALS AND METHODS

Membrane Production. A previously described method (7) was used. A co–cross-linking process was performed with 26.5 mg/ml plasma albumin, 2.5 mg/ml glutaraldehyde, 1.25 IU/ml uricase, and 2.5 IU/ml xanthine oxidase in a 0.02 M phosphate buffer at pH 6.8 (membrane thickness 50 μm).

Enzyme Activity Measurements. By measuring the inward substrate flux or the outward product flux for $[S] \gg K_m$, a determination of the maximal enzyme activity, V_M, was obtained for bound enzyme or for free enzyme in solution.

Xanthine Oxidase Activity. Xanthine is transformed into uric acid by xanthine oxidase (Sigma, from buttermilk) in the presence of molecular oxygen. Enzyme activity was obtained by measurement of the absorption at 293 nm ($\Delta\varepsilon = 1.2 \times 10^7$ cm^2 mol^{-1}).

Uricase Activity. Uricase activity (Sigma, from *Candida utilis*) was obtained by spectrophotometric measurement of substrate consumption ($\Delta\varepsilon = 1.2 \times 10^7$ cm^2 mol^{-1}).

For each enzyme, kinetic measurements were performed at pH 9.3 in a 0.05 M glycine NaOH buffer.

Bienzyme System. There is an isobestic point for xanthine and uric acid at 281 nm with $\Delta\varepsilon = 0.87 \times 10^7$ cm^2 mol^{-1}. Allantoin, the final product, does not give an absorption at this wavelength. The overall kinetics of the bienzyme system were measured spectrophotometrically at 281 nm. With simultaneous measurements at 281 and 300 nm, the concentrations of xanthine and uric acid could be determined (xanthine $\Delta\varepsilon$ at 300 nm: 0.09×10^7 cm^2 mol^{-1}; uric acid $\Delta\varepsilon$ at 300 nm; 0.98×10^7 cm^2 mol^{-1}).

Permeability Measurements. Diffusion through the membrane was studied using a diffusion cell in which the film under investigation separated two compartments.

The same cell was used to study time-dependent fluxes and concentrations with different substrates in each compartment, separated by a membrane bearing enzyme activities. The solutions in each compartment flowed continuously through spectrophotometer cuvettes. The absorptions at

281 nm and 300 nm were recorded simultaneously in order to follow the variation of concentrations.

THEORETICAL SECTION

The previously introduced bienzyme system is:

$$I \xrightarrow{E_1} S \xrightarrow{E_2} P$$

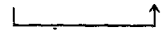

Competitive inhibition

$[S]$ is the substrate concentration, $[I]$ is the inhibitor concentration; V_1 and V_2 are maximum enzyme activities for E_1 and E_2; K_{m_1} and K_{m_2} are Michaelis constants for E_1 and E_2; K_I is the inhibition constant.

Enzyme Membrane System. Michaelian kinetics do not apply globally in heterogeneous systems. Nevertheless, the Michaelian expression of enzyme activity is valid for an *elementary volume.*

For every substance A with concentration $[A]=[A](x, t)$, and for every point inside the membrane, $(\partial[A]/\partial t)$ is linked to enzyme reaction and metabolite diffusion by

$$\frac{\partial[A]}{\partial t}=\left(\frac{\partial[A]}{\partial t}\right)_{\text{diffusion}}+\left(\frac{\partial[A]}{\partial t}\right)_{\text{reaction}}$$

The statement of Fick's second law is:

$$\left(\frac{\partial[A]}{\partial t}\right)_{\text{diffusion}}=D_a\frac{\partial^2[A]}{\partial x^2}$$

where x refers to the distance from the origin in a perpendicular direction to the membrane surface and D_a is the diffusion coefficient of substance A.

Accordingly, the continuity equations for I, S, and P inside the membrane can be written:

$$\frac{\partial[I]}{\partial t}=D_I\frac{\partial^2[I]}{\partial x^2}-V_1\frac{[I]}{K_{m_1}+[I]} \tag{1}$$

$$\frac{\partial[S]}{\partial t}=D_S\frac{\partial^2[S]}{\partial x^2}+V_1\frac{[I]}{K_{m_1}+[I]}-V_2\frac{[S]}{[S]+K_{m_2}(1+[I]/K_I)} \tag{2}$$

$$\frac{\partial[P]}{\partial t}=D_P\frac{\partial^2[P]}{\partial x^2}+V_2\frac{[S]}{[S]+K_{m_2}(1+[I]/K_I)} \tag{3}$$

By using dimensionless parameters with the thickness e, e^2/D_I, and K_{m_2} as space, time, and concentration units, equations (1), (2), and (3) can be written as:

$$\frac{\partial i}{\partial t} = \frac{\partial^2 i}{\partial x^2} - \sigma_1 \frac{i}{i + (K_{m_1}/K_{m_2})}$$

with

$$\sigma_1 = \frac{V_1}{K_{m_2}} \frac{e^2}{D_I}$$

$$\frac{\partial s}{\partial t} = \frac{D_S \partial^2 s}{D_I \partial x^2} + \sigma_1 \frac{i}{i + (K_{m_1}/K_{m_2})} - \sigma_2 \frac{s}{s + 1 + (K_{m_2}/K_I) i}$$

with

$$\sigma_2 = \frac{V_2}{K_{m_2}} \frac{e^2}{D_I}$$

$$\frac{\partial p}{\partial t} = \frac{D_p}{D_I} \frac{\partial^2 p}{\partial x^2} + \sigma_2 \frac{s}{s + 1 + (K_{m_2}/K_I) i}$$

Boundary conditions for I *and* S

The boundary concentrations are not constrained, so that:

(a) $$\frac{\partial i}{\partial t} + \chi \frac{\partial i}{\partial v} = 0$$

where

$$\frac{\partial}{\partial v} = \begin{cases} -\dfrac{\partial}{\partial x} \text{ for } x = o \\ \\ +\dfrac{\partial}{\partial x} \text{ for } x = e \end{cases}$$

and

$$\chi = \frac{\Omega e}{V}$$

with Ω the area of the membrane–solution interface, and V the volume of solution in each compartment.

Initial conditions are:

$$i(o, o) = o$$

$$i(e, o) = \frac{I_o}{K_{m_2}}$$

(b) Boundary conditions for S are the same with the following initial conditions

$$s(o, o) = s(e, o) = \frac{S_o}{K_{m_2}}$$

These nonlinear partial differential equations systems can be solved numerically on a computer (15).

Numerical results will be given together with the experimental data.

EXPERIMENTAL AND NUMERICAL RESULTS

The results given in Fig. 1 deal with a monoenzyme membrane (uricase) studied under symmetrical conditions for substrate (10^{-7} mol cm^{-3} on both sides) and asymmetrical conditions for inhibitor (respectively, 0 in compartment 1 and 1.4×10^{-7} mol cm^{-3} in compartment 2).

Due to the enzyme reaction, substrate molecules are entering the membrane on both sides. The flux is leaving compartment 2. There is a quantitative difference from classic experiments dealing with an immersed enzyme membrane (14), but qualitatively the behavior is similar: Substrate molecules are consumed on both sides of the membranes.

With a homogeneous bienzyme membrane (xanthine oxidase–uricase), a qualitatively different behavior is observed (Figs. 2 and 3). Under the boundary conditions for substrate and inhibitor described above, urate molecules are leaving and entering the membrane by the first and the second

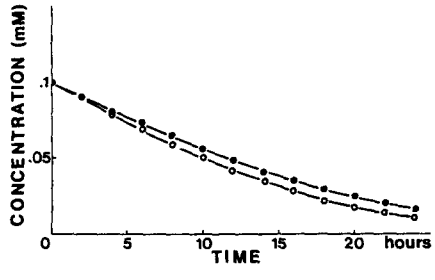

FIG. 1. Time-dependent evolution of uric acid concentrations for a monoenzyme membrane (uricase) working between two compartments: 1 (○) and 2 (●). Initial concentrations for xanthine are 0 and 1.4×10^{-7} mol cm^{-3} in compartments 1 and 2, respectively.

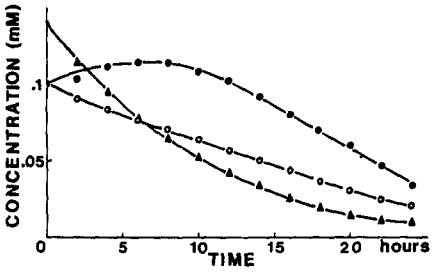

FIG. 2. Time-dependent evolution of uric acid concentrations for a bienzyme membrane (xanthine oxidase-uricase) between two compartments: 1 (○) and 2 (●). Xanthine concentration is given for compartment 2 (▲); the concentration in compartment 1 remains equal to zero. Initial conditions for uric acid and xanthine are the same as in Fig. 1.

side, respectively. The urate concentration is decreasing in the first compartment and increasing in the second (Fig. 2). In this way, a concentration gradient is generated between the membrane boundaries. The entering and leaving fluxes measured experimentally are given as a function of time in Fig. 3.

The concentration evolution in both compartments was calculated numerically on a computer by using the basic parameter values of the system and the equations previously introduced (Fig. 4). A good agreement is observed between experimental and numerical results.

The behavior of the mono- and bienzyme systems is explained by the membrane concentration profiles calculated numerically. Substrate concentrations are given in Fig. 5A as a function of the abscissa in the membrane. The flux at each point is proportional to the slope of the profile. For V_1 (xanthine oxidase), values are equal to or greater than 0.8×10^{-4} mol cm^{-3} h^{-1}. Slopes at both membrane boundaries are of the same sign: Substrate molecules enter at one side and leave at the other. The global behavior is explained physicochemically by the existence of two parts in the membrane with a concentration lower and higher, respectively, than the

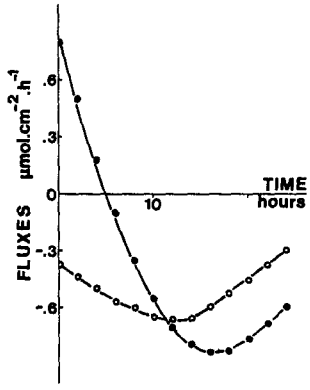

FIG. 3. Measured fluxes as a function of time for uric acid in compartments 1 (○) and 2 (●) for the bienzyme membrane system during the Fig. 2 experiment.

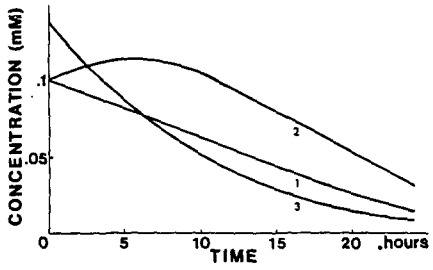

FIG. 4. "Simulation on the computer." Calculated time-dependent evolution of uric acid concentration in compartment 1 (curve *1*) and 2 (curve *2*); xanthine concentration in compartment 2 (curve *3*) for the bienzyme membrane system. The computation was performed with the following parameter values:

$V_1 = 1.4\times10^{-4}$ mol cm^{-3} h^{-1};

$V_2 = 0.5\times10^{-4}$ mol cm^{-3} h^{-1};

$D_I = 2.7\times10^{-3}$ cm^2 h^{-1};

$D_S = 2.5\times10^{-3}$ cm^2 h^{-1};

$K_{m1} = 2\times10^{-8}$ mol cm^{-3};

$K_{m2} = 4\times10^{-8}$ mol cm^{-3};

$K_I = 2\times10^{-8}$ mol cm^{-3};

$e = 5\times10^{-3}$; $V = 30$ cm^3;

$\Omega = 2.5$ cm^2

These parameter values are the same as in Fig. 2.

concentration of the bulk solution. The homogeneous bienzyme membrane gives rise to a global vectorial effect with asymmetrical boundary conditions. Figure 5B shows the evolution of substrate profiles as a function of time when the system is starting under pseudoactive transport conditions ($V_1 = 1.4\times10^{-4}$ mol cm^{-3} h^{-1}). These profiles deal with the experiments described in Figs. 2 and 4.

CONCLUSION

The studies dealing with immobilized enzymes were mainly performed under asymmetrical boundary conditions. Within biological systems,

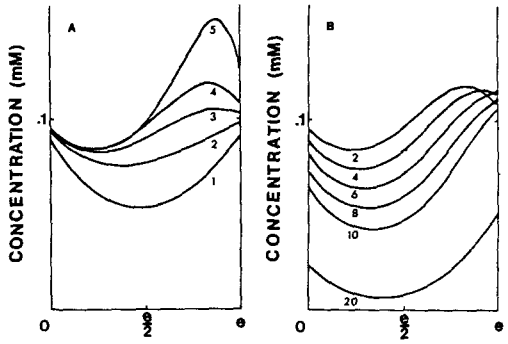

FIG. 5(A) Concentration profiles of uric acid inside the membrane under stationary state conditions for constant V_{m2} values (0.5×10^{-4} mol cm^{-3} h^{-1}) and for different V_{m1} values (*1*:0; *2*:0.4×10^{-4}; *3*:0.8×10^{-4}; *4*:0.14×10^{-3}; *5*:0.5×10^{-3} mol cm^{-3} h^{-1}). For profiles *3*, *4*, and *5*, a pseudoactive transport effect is observed: $S_1 < S_2$, and uric acid molecules are entering and leaving compartments 1 and 2, respectively. (B) Concentration profiles of uric acid inside the membrane during evolution (2, 4, 6, 8, 10, and 20 hours) for system starting under pseudoactive transport conditions.

immobilized enzymes are often working between compartments bearing different metabolite concentrations. The film shape allows a study of the enzyme behavior under asymmetrical boundary conditions in a well-defined context (7, 16).

The asymmetrical conditions are able to generate some vectorial behaviors. The vectorial catalysis deals with two kinds of phenomena: (1) the asymmetry in the structure of the membrane itself or (2) the asymmetry in the function created by a gradient between the boundaries of a membrane homogeneous in structure.

The results described deal with the last aspect. A bienzyme membrane that is homogeneous in structure becomes heterogeneous in function. A vectorial behavior is observed: Due to the asymmetrical substrate concentration profile in the membrane a pseudoactive transport effect occurs. A global mass transfer of substrate across the membrane without or against the concentration gradient is observed. The system is an example of a vectorial catalysis effect within a defined context. The results could be useful for the explanation of the behavior of biological membranes in which facilitated or active transport is observed. The simulation on the computer is in good agreement with the experimental results. Evidence for the explanation of a vectorial catalysis in terms of diffusion-reaction is given.

REFERENCES

1. BLUMENTHAL, R., CAPLAN, S. R., and KEDEM, O. (1967) Biophys. J. 7 : 735.
2. DAVID, A., METAYER, H., THOMAS, D., and BROUN, G. (1974) J. Membr. Biol. 18 : 113.
3. BROUN, G., THOMAS, D., and SELEGNY, E. (1972) J. Membr. Biol. 8 : 313.
4. WEISZ, P. B. (1973) Science 179 : 433.
5. SILMAN, M. I., and KATCHALSKI, E. (1966) Annu. Rev. Biochem. 35 : 873.
6. GRYSZKIEWICK, J. (1971) Folia Biol. (Krakow) 19 : 119.
7. THOMAS, D., BROUN, G., GELLF, G., and DOMURADO, D. (1972) Biotechnol. Bioeng. Symp. 3 : 299.
8. MOSBACH, K., and MATTIASSON, B. (1970) Acta Chem. Scand. 24 : 2093.
9. MATTIASSON, B., and MOSBACH, K. (1971) Biochem. Biophys. Acta 235 : 253.
10. SRERE, P. A., MATTIASSON, B., and MOSBACH, K. (1973) Proc. Natl. Acad. Sci. U.S.A. 70 : 2534.
11. GOLDMAN, R., and KATCHALSKI, E. (1971) J. Theor. Biol. 32 : 243.
12. HERVAGAULT, J. F., JOLY, G., and THOMAS, D. (1975) Eur. J. Biochem. 51 : 19.
13. LECOQ, D., HERVAGAULT, J. F., BROUN, G., JOLY, G., KERNEVEZ, J. P., and THOMAS, D. (1975) J. Biol. Chem. 250 : 5496.
14. THOMAS, D., BOURDILLON, G., BROUN, G., and KERNEVEZ, J. P. (1974) Biochemistry 13 : 2995.
15. KERNEVEZ, J. P., and THOMAS, D. (1975) J. Appl. Math. Optim. 1 : 222.
16. GOLDMAN, R., KEDEM, D., and KATCHALSKI, E. (1968) Biochemistry 7 : 4518.